Supporting information

Understanding Metal Organic Chemical Vapour Deposition of Monolayer WS_2: The Enhancing Role of Au Substrate for Simple Organosulfur Precursors

Ye Fan,#,† Kenichi Nakanishi,#,† Vlad P. Veigang-Radulescu,† Ryo Mizuta,† Callum Stewart,† Jack E. N. Swallow,‖ Alice Dearle,† Oliver Burton,† Jack A. Alexander-Webber,† Pilar Ferrer-Escorihuela,§ Georg Held,§ Barry Brennan,‡ Andrew J. Pollard,‡ Robert S. Weatherup,‖ Stephan Hofmann†, *

† Electrical Engineering Division, Department of Engineering, University of Cambridge

‡ National Physical Laboratory, Hampton Rd, Teddington, Middlesex, TW11 0LW, United Kingdom

‖ Department of Materials, University of Oxford, Parks Road, Oxford OX1 3PH, United Kingdom

§ Diamond Light Source Ltd., Harwell Science and Innovation Campus, Didcot OX11 0DE, United Kingdom

Contributed equally

* Corresponding author

ToF-SIMS depth profile of post-growth samples (figure S1):

More data is provided for the depth profile of as-grown WS_2 on gold. The sample in figure S1 (a) is sulfurized under 0.3 mbar DMS and the sample in figure S1 (b) is sulfurized under 1 mbar DMS.

To detect the distribution of different elements in the 'bulk' Au, 10 keV Cs^+ ions are used for sputtering. Here 'bulk' refers to Au foil that is more than ~10 nm below the surface. The Cs^+ sputter allows us to detect W, S, O, and C up to ~400 nm depth from the surface. As shown in figure S1 (a, i) and (b, i), the distribution of these element in bulk Au is not strongly influenced by the growth condition. This confirms our theory that the catalytic reaction is

surface limited. Moreover, both S and W diminish from surface to bulk, which is due to the low thermal equilibrium solubility of both elements in Au.

Figure S1 also provides the results measured by 10 keV Ar_{2700}^{+} ion sputtering, in which the measurement is confined to only the top ~20 nm from the surface. The distributions of carbon and WS_2 versus sputter time have been shown in figure 5 (d) and (e) in main text, but further results are shown here in figure S1 (a, ii) and (b, ii). The carbon concentration sensitively depends on the partial pressure of DMS during the sulfidation step as reported in the main text and figure 5 (d) and (e).

ToF-SIMS images over millimeter range (figure S2):

Additional ToF-SIMS data on MOCVD WS_2 and its dependence on sulfidation pressure are provided in figure S2. To confirm the continuity and uniformity of MOCVD WS_2 on gold, ToF-SIMS mapping is carried out at the millimetre scale (5 mm × 5 mm). The samples are grown with (a) 0.1 mbar and (b) 1 mbar DMS partial pressure during the sulfidation step, respectively. The ToF-SIMS C_2^- ion signal is shown in (c), comparing carbon contamination levels between the two process conditions. In samples grown with high DMS exposures, a significant amount of carbon can be detected by ToF-SIMS in the same location as WS_2.

Transfer curve and light response of WS_2 (figure S3):

A WS_2 field effect transistor (FET) is fabricated on 300nm SiO_2 on P-doped silicon to measure the field effect mobility. A 2-terminal device structure is used. In (20 nm)/Au (80 nm) is evaporated as source and drain contact for all the devices. After the device fabrication, the chip is encapsulated by 10 nm of atomic layer deposited (ALD) Al_2O_3 to prevent degradation. The device is current-annealed by high source-drain bias (10 V) for multiple cycles until the transfer curve does not change. All measurements are carried out at room

temperature under ambient environment. A halogen lamp (λ_{peak} ~ 906 nm, I ~ 0.03 Wcm^{-2}) with a manual switch is used to test the light response of the sample.

The FET mobility is measured by fitting the linear region (marked by the dashed lines in figure S3 b) in the transfer curve of the WS_2 FET (as shown in figure S3). The field effect mobility of WS_2 is measured as 0.51 $cm^2V^{-1}s^{-1}$ in light and 0.40 $cm^2V^{-1}s^{-1}$ in dark. However, the threshold voltage does not change very much with and without light, i.e. 29.2 V in light and 30.4 V in dark. The subthreshold swing is measured as 15.8 V/dec in dark and 16.6 V/dec in light.

XPS of carbon contamination from long-time DMS exposure (figure S4):

The reaction between W and DMS is marked by a shift to higher binding energies and broadening of the W 4f peaks as discussed in the main text and below. However, after the sulfidation of W to WS_2 finished, the deposition of amorphous carbon (not tungsten carbide) continues. As shown in figure S4, the carbon intensity keeps on increasing even after the W 4f peak no longer displays any changes. Additionally, we notice that while the amorphous carbon XPS signal increases throughout the experiment, at some point the WC signal remains the same intensity, suggesting a similar saturation point to that of WS_2 formation.

XPS of W4f before and after sulfidation (figure S5):

To highlight the change of W 4f peak positions, we overlay spectra taken during the metallization and the sulfidation steps in figure S5. These data are normalized to their maximum intensity for better comparison. The peak maxima are shifted by around ~0.4 eV to higher binding energies going from metallic W to W(IV). This is accompanied by a slight broadening of the peaks, from 1.0 eV to 1.2 eV. A difference spectrum is employed to assist in visualizing the relevant differences between the core levels, and indicate possible

components that can be incorporated into the fitting of the data. Some intensity is lost around 31.3 eV following sulfidation compared to the metallic data, while a gain in spectral intensity at ~32.1 eV emerges. We expect, with the strong overlap between the peaks, that not all W is converted to WS_2 (supported by the fitting applied to the data in figure 3e of the main manuscript and further rationale within the manuscript). Hence, the reduction in intensity for the WS_2 compared to W by no means indicates a complete transformation to WS_2, nor a complete loss of metallic W during sulfidation. However, the gain in intensity at 32.1 eV is consistent with the formation of a second species (WS_2), which is supported by the slight broadening of peaks. Indeed, this is further supported by the fitting procedure in the main manuscript.

SEM of WS_2 on Au (figure S6):

WS_2 can also be grown by sulfurizing a pre-patterned W pad as shown in figure S6 (a). The W pad is about 300nm thick. WS_2 is found in a dendritic pattern (but still attached to Au surface) around the W pad, which indicates a finite mobility of W atoms on the Au surface at the temperature of reaction. Figure S6 (b) is a high-magnification SEM image of a single WS_2 domain. This sample is grown with a short DMS exposure time (~2 min) so that the WS_2 is not continuous. Unreacted W particles can be found in the image. Moreover, it is interesting to note that the WS_2 domain follows the terrace of gold at the early stages of growth. Such substrate-controlled growth is commonly found in graphene growth on e.g. Pt, but rarely found in WS_2 grown on inert substrate like SiO_2 or sapphire. When most regions of Au are covered by the WS_2 film, the sulfidation reaction is largely inhibited, which leads to a self-limitation growth manner. A micro-crack, where two WS_2 domains are not fully merged, is shown in figure S6 (c). We notice that the excessive tungsten on the as-grown WS_2 film tends to remain as particles instead of being converted to a 2^{nd} layer of WS_2.

Particles on as-transferred WS_2 film (figure S7)

Particles can be found on the transferred WS_2 film as shown in figure S7. The WS_2 film is grown as described in the main text, with 0.1mbar DMS partial pressure used during sulfidation. After the growth, WS_2 is transferred onto a silicon chip with a 300 nm oxide layer for AFM characterisation. Another sample grown at the same conditions was transferred to a TEM grid. The details of transfer and TEM set-ups are described in the main text. The as-transferred WS_2 film is decorated with nano particles as shown in figure S7 (a) and (b). Similar particles are also found on WS_2 before transfer, see figure S6 (b) and (c). These particles most likely originate from residual tungsten that does not fully convert to WS_2 during the sulfidation reaction.

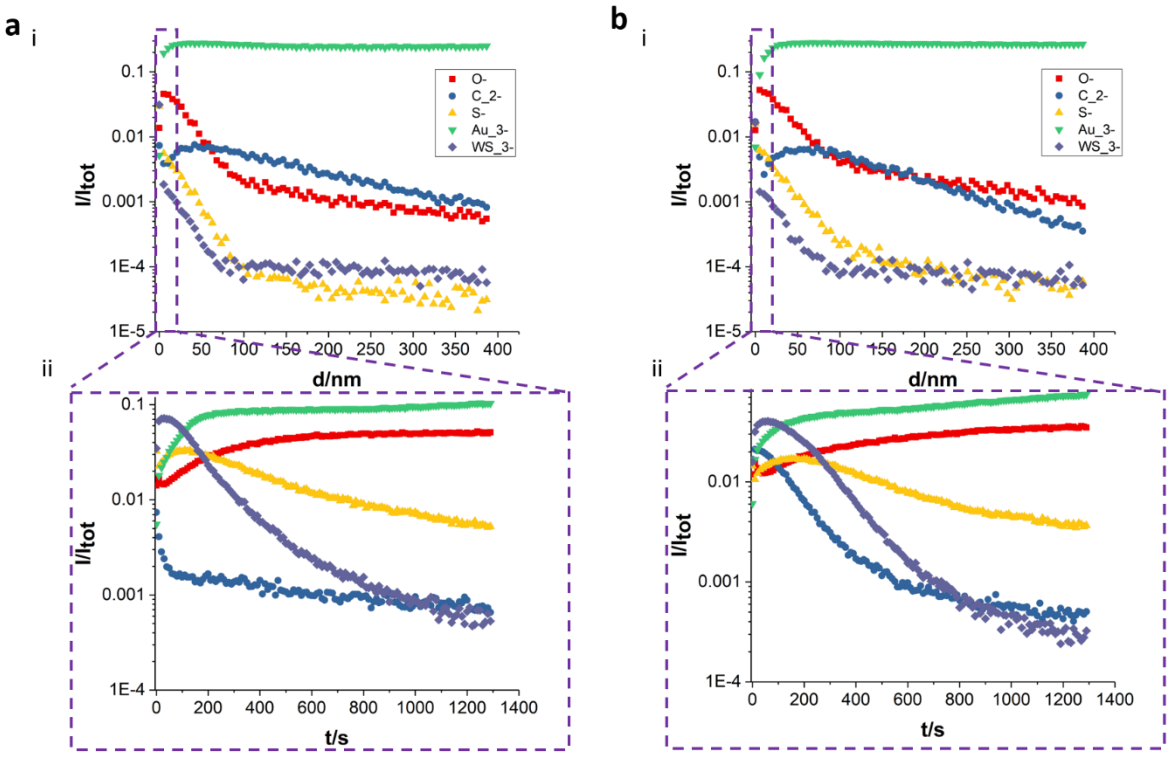

Figure S1. ToF-SIMS depth profiles of different ion species*. (a) Depth profile taken on WS_2 grown by 0.3 mbar DMS sulfidation and (b) on WS_2 grown by 1 mbar DMS sulfidation. In both cases (i) shows the course depth profile up to 400 nm into the Au, sputtered by 10 keV Cs+ ions and (ii) shows depth profiles from the surface regions, sputtered by 10 keV Ar2700+ ions.*

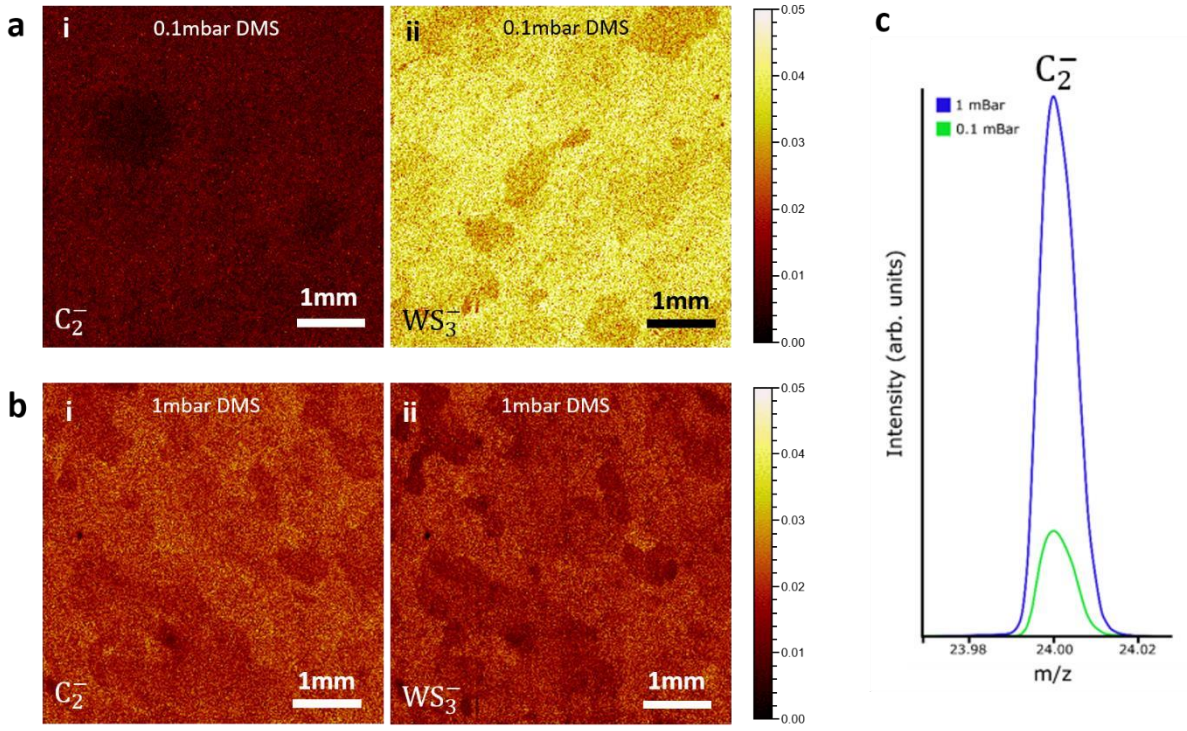

Figure S2. Large area (5 mm × 5 mm) ToF-SIMS imaging of WS_2. *(a) SIMS surface maps of WS_2 grown with 0.1 mbar DMS during sulfurization. The ion intensity of both C_2^- (a, i) and WS_3^- (a, ii) are normalized to the total ion intensity. (b) SIMS surface maps of WS_2 grown with 1 mbar DMS during sulfidation. The ion intensity of both C_2^- (b, i) and WS_3^- (b, ii) are normalized to the total ion intensity. (c) ToF-SIMS ion signal of C_2^- comparing the relative carbon content on the surface of both samples. In samples grown with high DMS partial pressure, a significant increasing of carbon can be detected.*

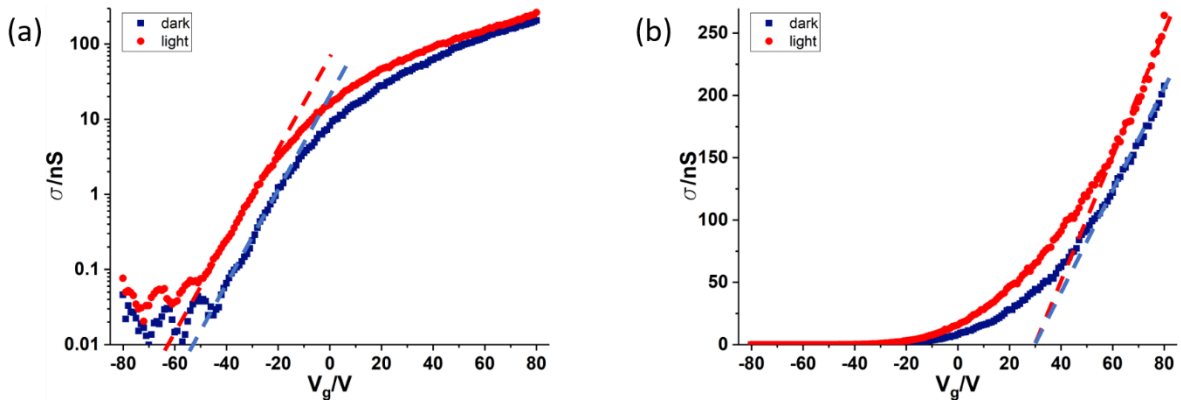

Figure S3. Transfer measurement of WS_2. *(a) Semi-log plot. (b) Linear plot. The WS_2 shown an field-dependent light responsivity as shown by the difference between its transfer curve measured in dark (blue) and measured with light (red).*

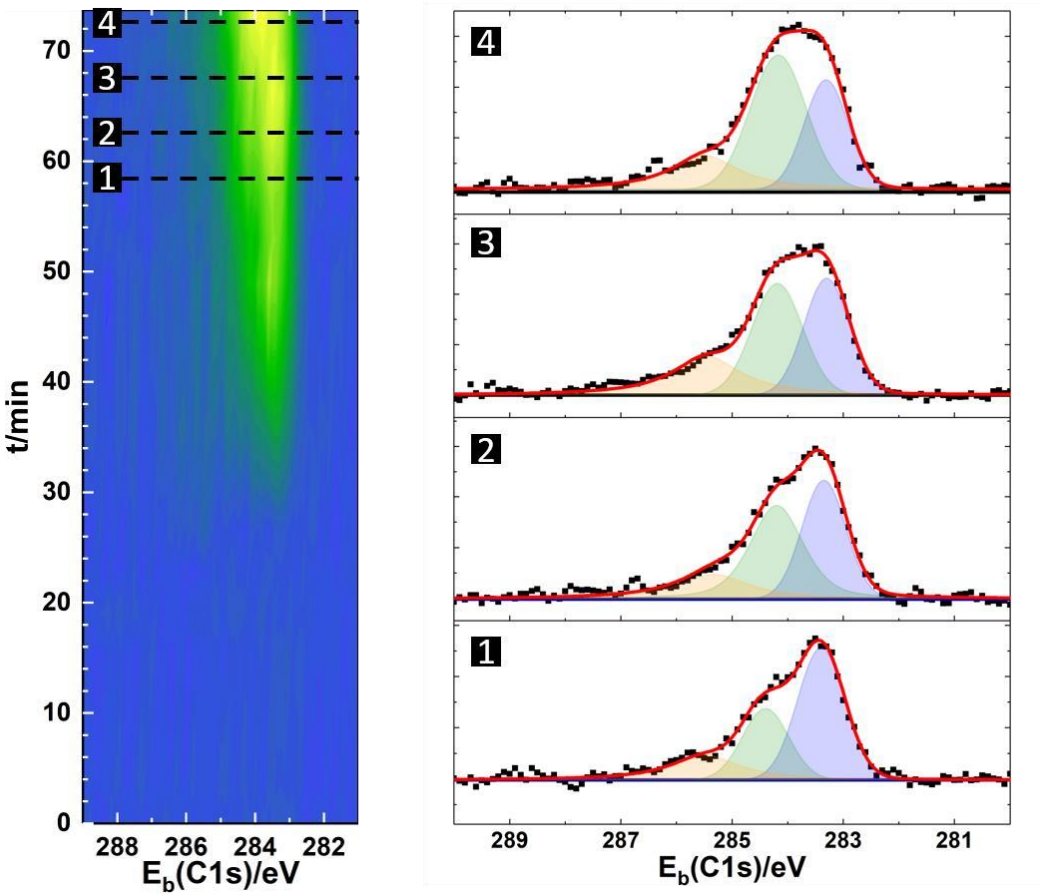

Figure S4. XPS of carbon species deposited during DMS exposure. *The left panel is the XPS intensity map of C 1s core level. The right panel show the XPS spectrum taken at different times. C 1s core level is consisted of three major components, which are tungsten carbide (blue), sp^2 carbon (green), and sp^3 carbon (orange).*

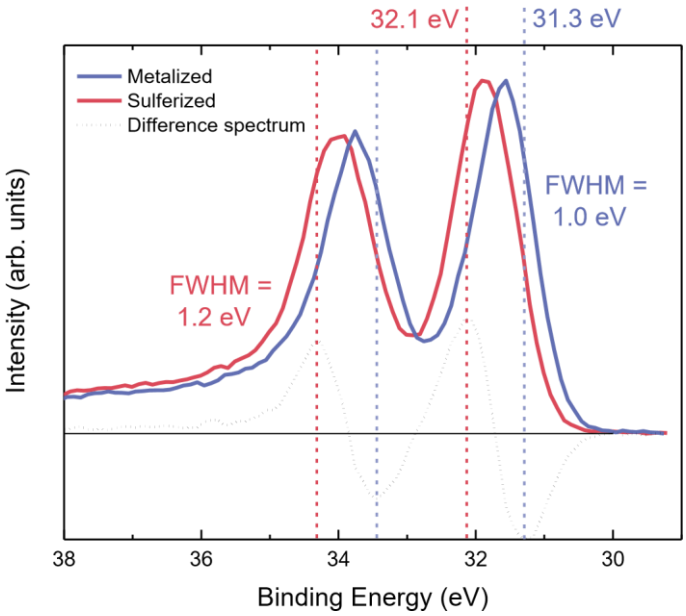

Figure S5. XPS of the W 4f region during the metallization step and the subsequent sulfidation step. *Peaks are normalized to the maximum intensity of the W $4f_{7/2}$ and a difference spectrum is displayed to aid in visualizing the change in the spectrum.*

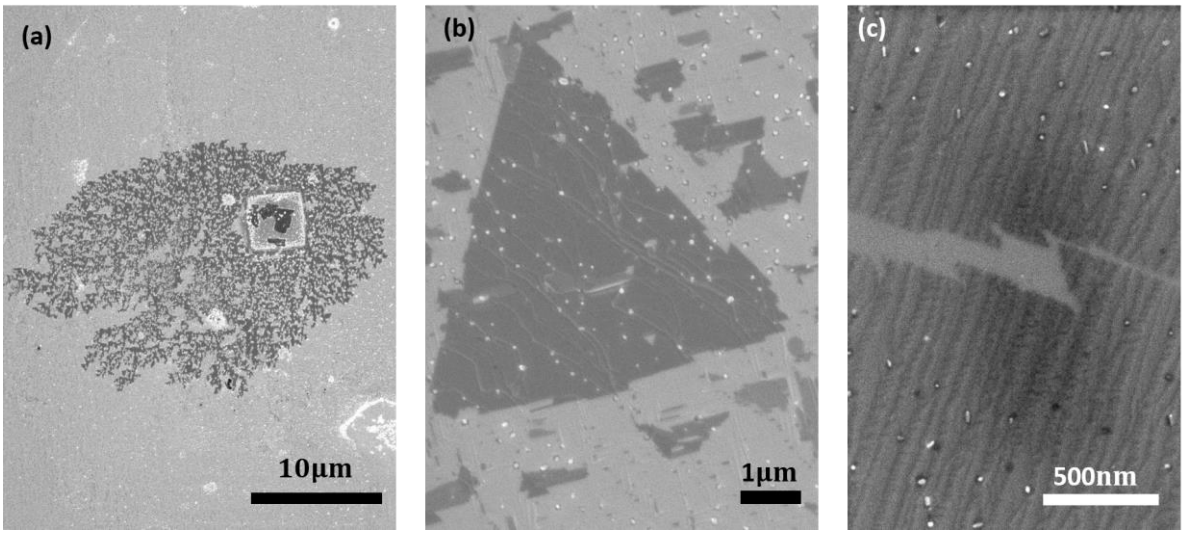

Figure S6. SEM images of WS_2 on Au. *(a) WS_2 around a square-shaped W pad on Au. Dendritic WS_2 grows around the W pads after sulfidation. (b) WS_2 domain grown with short DMS exposure. (c) Crack in the WS_2 film. Some WS_2 domains are not fully merged even after the formation of WS_2 film. Unreacted tungsten particles are visible in images (b) and (c).*

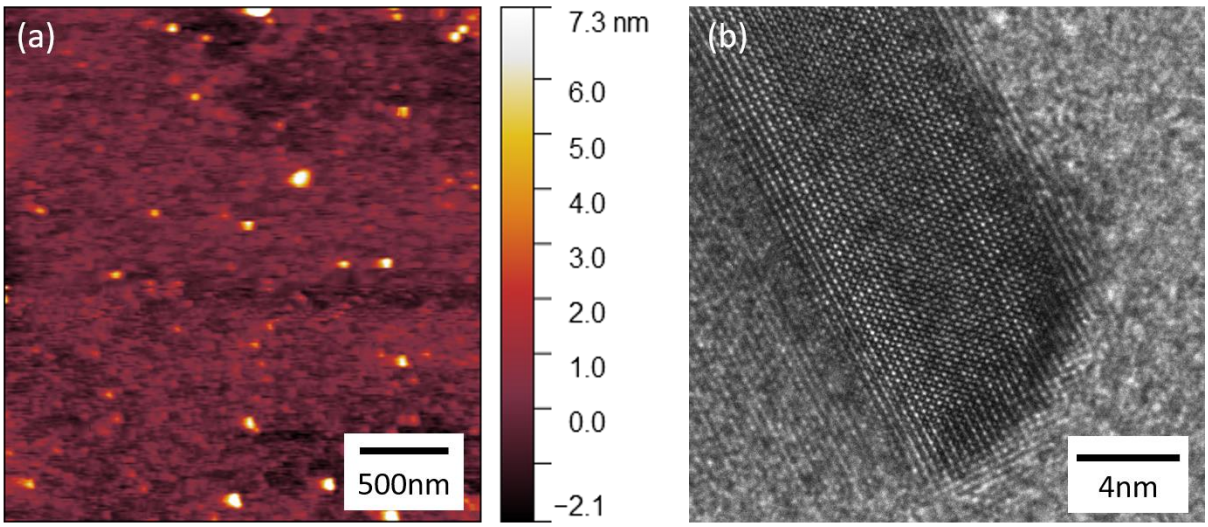

Figure S7. Characterisation of particles on as-transferred WS_2 *(a) AFM image of as-transferred WS_2 film on SiO_2. (b) HRTEM image of the particles on WS_2. The particle residuals originate from excess tungsten.*